Talanta 232 (2021) 122447

Contents lists available at ScienceDirect

Talanta

journal homepage: www.elsevier.com/locate/talanta

Disposable electrochemical microfluidic device for ultrasensitive detection of egg allergen in wine samples

Thaísa Aparecida Baldo [a], Camila dos Anjos Proença [a], Fabiana da Silva Felix [b], Tayane Aguiar Freitas [a], Solange Kazumi Sakata [c], Lúcio Angnes [d], Ronaldo Censi Faria [a,*]

[a] Departamento de Química, Universidade Federal de São Carlos, 13565-905, São Carlos, São Paulo, Brazil
[b] Departamento de Química, Universidade Federal de Lavras, CEP, 37200-900, Lavras, Minas Gerais, Brazil
[c] Centro de Tecnologia das Radiações – Instituto de Pesquisa Energéticas e Nucleares (IPEN/CNEN-SP), CEP, 05508-000, São Paulo, São Paulo, Brazil
[d] Instituto de Química, Universidade de São Paulo, CEP, 05508-000, São Paulo, São Paulo, Brazil

ARTICLE INFO

Keywords:
OVA detection
Immunoassay ultrasensitive detection
Disposable microfluidic platform

ABSTRACT

Food allergies have been increasing all over the world. Egg is an important component in the food industries and the second most common cause of food allergy, shortly after milk. In the wine industry, egg white is applied as a fining agent for tannin removal. In this study, a sandwich-based immunoassay for ultrasensitive detection of ovalbumin (OVA) in wine samples was developed. The assay involves the use of magnetic beads (MBs) decorated with a polyclonal anti-OVA antibody (Ab_2) and horseradish peroxidase (HRP), used as label for the quantification in a disposable electrochemical microfluidic device (DEμD) here developed. The Ab_2-MB-HRP prepared was applied to capture, separate, and pre-concentrate OVA from wine samples. In the DEμD, OVA was immune-magnetically captured (OVA-Ab_2-MB-HRP), producing a sandwich structure (GO-Ab_1-OVA-Ab_2-MB-HRP) on the electrode's surface. This arrangement results in an ultrasensitive device, achieving the ultralow limit of detection of 0.2 fg mL^{-1} OVA. Five samples of wines were analyzed by using the immuno-magneto-assay which presents excellent accuracy compared with enzyme-linked immunosorbent assay (ELISA).

1. Introduction

Food allergy is an uncommon response to a specific food triggered by the body's immune system. The symptoms may range from mild signs, beginning with eczema, difficulty breathing, stomach pain, vomiting, diarrhea, and anaphylaxis and in extreme cases leading to death. Foods that are responsible for the majority of allergic reactions are cow's milk, eggs (mainly egg white), seafood, soy, peanuts, tree nuts, and wheat, in which the allergenic agents are mainly proteins [1–3].

One of the allergen compounds that can be found in wine are proteins. During the wine fining, products from egg (ovalbumin or conalbumin), fish collagen, horse gelatins, and cow's milk can be used as processing aids substances [3]. These products promote the clarification of wines, through precipitation of polyphenols and tannin compounds, improving their gustatory characteristics. The complex species formed with the protein and polyphenols and tannins are removed by decantation or filtration steps [3–5]. However, traces of these allergenic proteins may remain in the wine, which can cause significant allergic reactions in sensitive consumers. The utilization of egg products is regulated in the USA by the Food and Drug Administration to protect consumers from the potential consequences of egg consumption. Allergen labeling is still required by law in many countries [6,7].

Enzyme-linked immunosorbent assay (ELISA) is the mostly applied method for protein detection, largely used in clinical diagnosis [8–13]. ELISA test is also used for monitoring proteins as allergenic compounds in food samples. However, in addition to requiring qualified personnel, in some cases ELISA tends to provide only semi-quantitative information, or else it does not have enough sensitivity for the allergen detection in some foods [14,15]. Methods based on liquid chromatography coupled with mass spectrometry (LC-MS and LC-MS/MS) have emerged as alternative methods for food allergen analysis and allowed full identification and determination of different allergens simultaneously [16,17]. However, these techniques require time-consuming sample preparation, elaborated data analysis, and relatively expensive instrumentation.

Electrochemical immunosensors constitute an interesting alternative for protein detection because of its high sensitivity, simplicity, and low-cost. The recent advances and different applications of electrochemical

* Corresponding author.
E-mail address: rcfaria@ufscar.br (R.C. Faria).

https://doi.org/10.1016/j.talanta.2021.122447
Received 2 February 2021; Received in revised form 16 April 2021; Accepted 17 April 2021
Available online 1 May 2021
0039-9140/© 2021 Elsevier B.V. This article is made available under the Elsevier license (http://www.elsevier.com/open-access/userlicense/1.0/).

immunosensors, including food analysis, have been recently reviewed [18]. Electrochemical sensors based on using 2D material as graphene have generated great interest because of their excellent properties such as faster electron transfer kinetics, lower limits of detection, and higher sensitivities than conventional carbon-based compounds [19–21]. Graphene oxide (GO) is a chemically modified graphene containing oxygen functional groups such as hydroxy, epoxy, and carboxylic groups, that are important groups for anchoring proteins and genetic materials as DNA and RNA as key biocompounds for biosensor construction [19,20,22].

Herein, a magnet-immunoassay based on the use of disposable electrochemical devices is described and applied for ultrasensitive detection of protein allergen in wine samples. The immunosensing platform here developed allowed simple and fast determination of ovalbumin with remarkable sensitivity showing excellent correlation with ELISA. The microfluidic device proposed can be easily produced with scalability, showing interesting properties as low-cost, disposability, portability, low requirements of reagents and samples.

2. Experimental

2.1. Reagents and materials

Magnetic beads Dynabead MyOne Carboxylic Acid with diameter and concentration of 1.0 μm and 10 mg mL^{-1}, respectively, were bought from Invitrogen (Vilnius, LT, USA). Graphite powder (grade#38) was obtained from Fisher Scientific (Hampton, VA, USA). For ELISA, goat anti-rabbit IgG were obtained from Abcam (Portsmouth, NH, USA). The wine samples were acquired at a local market. All the following reagents were purchased from Sigma Aldrich (St. Louis, MO, USA): poly(diallyldimethylammonium chloride) solution (PDDA, 20% wt% in H_2O), horseradish peroxidase (HRP), polyethylene glycol sorbitan monolaurate (Tween-20); 2-(N-Morpholino) ethanesulfonic acid hydrate (MES), hydroquinone (HQ), bovine serum albumin (BSA), hydrogen peroxide solution (30% w/w in H_2O), glycine, N-Hydroxysuccinimide (NHS), 4-(2-hydroxyethyl)-1-piperazineethanesulfonic acid (HEPES), N-(3-Dimethylaminopropyl)-N′-ethylcarbodiimide hydrochloride (EDC), sodium borohydride, γ-L-Glutamyl-L-cysteinyl-glycine (L-glutathione reduced, GSH), gold (III) chloride hydrate, monoclonal (mouse) primary antibody (Ab_1) to ovalbumin (OVA), polyclonal (rabbit) secondary antibody to OVA (Ab_2), ovalbumin (albumin from chicken egg white) (≥98% purity), tetramethylbenzidine (TMB), sulfuric acid, sodium nitrate, and potassium permanganate.

2.2. Instrumental

The electrochemical measurements were performed with a μSAT8000 Portable Multipotentiostat/Galvanostat from DropSens using Dropview 8400 software (Llanera, Spain). The microfluidic system was composed of a syringe pump (New Era), a manual chromatographic injection valve (Rheodyne, 7725i) with a sample loop of 100 μL, connected by polyether ether ketone (PEEK) tubes and fittings. The ELISA experiments were carried out using a Labtech Microplate Reader (LT-4000). A cutter machine from Silhouette Model Cameo Studio controlled by the Silhouette studio software v.3.8, was used for the construction of the disposable electrochemical device. All solutions used throughout this study were prepared with purified water obtained from a Millipore Milli-Q system with resistivity ≥18.2 MΩ cm (Bedford, MA, USA).

2.3. Synthesis of graphene oxide

The GO was prepared from graphite powder using a modified Hummers' method as previously reported [20]. The obtained GO was dispersed in ultrapure water (0.5 mg mL^{-1}) by sonication for a period of 2 h to obtain a stable brown dispersion. In sequence, the GO dispersion was centrifuged at 7000 rpm for 20 min and the excess of unoxidized graphite and the GO unexfoliated were removed [20].

2.4. Construction of the disposable electrochemical microfluidic device (DEμD) and the modification of the working electrodes

The microfluidic device developed for this study is presented in Fig. 1. The DEμD fabrication involves the use of screen-printing techniques that were detailed previously [23,24]. The electrodes layouts were created using the Silhouette studio software v.3.8 and the designed array was cut on the vinyl adhesive by Silhouette Model Cameo Studio cutter. The vinyl foil was placed over the cutting base of the cutter printer and the design of each electrode was cut out. In sequence, the undesirable parts were removed, and the vinyl adhesive was applied over a polyester sheet. In present design, 8 working carbon-based electrodes (8-WEs) were built with an exposed geometric area of 3.14 mm^2 each one (Fig. 1C). Carbon ink was applied using a screen-printing technique and subsequently cured for 30 min at 90 °C. Finally, the vinyl mask was removed and the foil with the electrodes was covered by the blue vinyl adhesive foil that was pressed using a heat press machine. In parallel to the preparation of the 8-WEs, the counter and reference electrodes were designed and assembled in a separated foil (Fig. 1 - A and B) also using screen-printed technique. After the carbon ink application, a layer of silver/silver chloride ink was applied on the pseudo-reference electrode, and cured for 30 min at 60 °C, followed by the vinyl layer removing.

The microfluidic channel was set up using a double-sided adhesive polystyrene card (Fig. 1D), in which a rectangular channel (45 mm × 4 mm) was cut using the electronic craft cutter (A3 Cutting Plotter, F1 Supplies, Brazil). The 8-WEs were positioned on one side and the counter and pseudo-reference electrodes on the other. The total volume of the microfluidic channel was approximately 75 μL.

The 8-WEs were initially modified with a bilayer electrostatically supported based on polycation PDDA and GO. Before assembling the DEμD, the 8-WEs were modified with the Ab_1, which was immobilized covalently [25]. The steps for the modification of the electrodes are depicted in Fig. 2A. For this, the 8-WEs were previously washed with water followed by the addition of 5 μL of 2.0 mg mL^{-1} PDDA in 0.05 mol L^{-1} NaCl. The electrodes were kept in this solution for 20 min. Next, the 8-WEs were rinsed with water, dried, and then 5 μL of a GO dispersion at 0.5 mg mL^{-1} was added to each electrode. The array was maintained overnight at room temperature to dry. The carboxyl groups connected to GO were activated by adding a freshly prepared aqueous solution composed of a mixture of EDC and NHS at 0.4 mol L^{-1} and 0.1 mol L^{-1}, respectively. The EDC/NHS reacted with the carboxyl groups in two steps, forming NHS ester, which was stable and effective for covalent conjugation to primaries antibodies [26]. After 20 min, the 8-WEs were rinsed and 5 μL of Ab_1 were added on the electrodes surface. The arrangement was kept overnight at 4 °C to complete the covalent immobilization, by the amide bonding formation between activated carboxyl group on GO and amine group on Ab_1. Then, the array of 8-WEs was washed with a saline PBS to remove the excess of material. In sequence, the remaining activated carboxyl groups were blocked by 2% (m/v) of BSA in PBS, which was kept in contact for 1 h at 4 °C, to avoid nonspecific binding reaction. Finally, the 8-WEs were washed with PBS, the DEμD was assembled and kept at 4° until use.

2.5. Bioconjugation of magnetic beads with polyclonal antibody and HRP

The HRP and the polyclonal anti-OVA antibody were conjugated in the magnetic beads as previously reported [23,24,27]. The steps for MBs decoration are represented in Fig. 2B. Initially, 200 μL of 10 mg mL^{-1} of MBs dispersion were transferred to a microtube containing 1.0 mL of 25 mmol L^{-1} of MES buffer (pH 6.0) and shaked in a vortex mixer for 30 s. Next, the MBs were washed three times with MES buffer, using a magnetic stand outside of the Eppendorf tube to retain the magnetic beads.

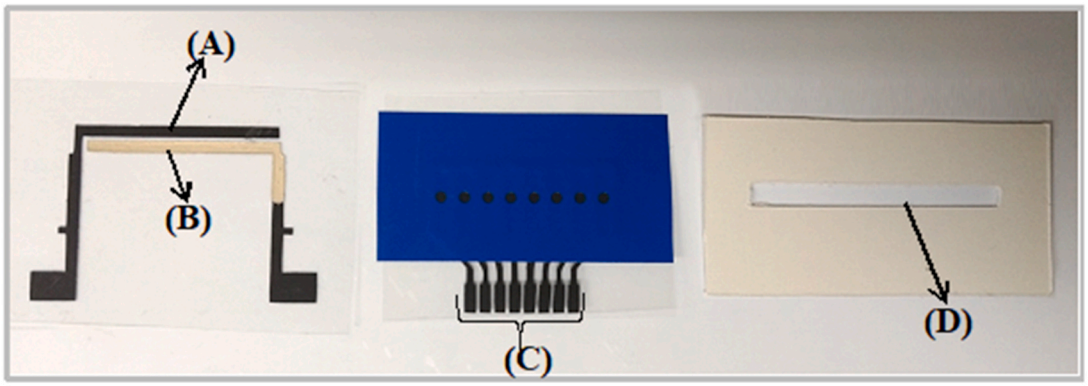


Fig. 1. Components of the DEμD: Left: Polyester sheet with (A) counter electrode, (B) Ag|AgCl pseudo-reference electrode; Center (C): Second polyester sheet with 8 carbon-based electrodes and a vinyl adhesive (blue) to define the exposed area of each electrode; and right: (D) a double-side adhesive polystyrene card with the microfluidic channel. (For interpretation of the references to color in this figure legend, the reader is referred to the Web version of this article.)

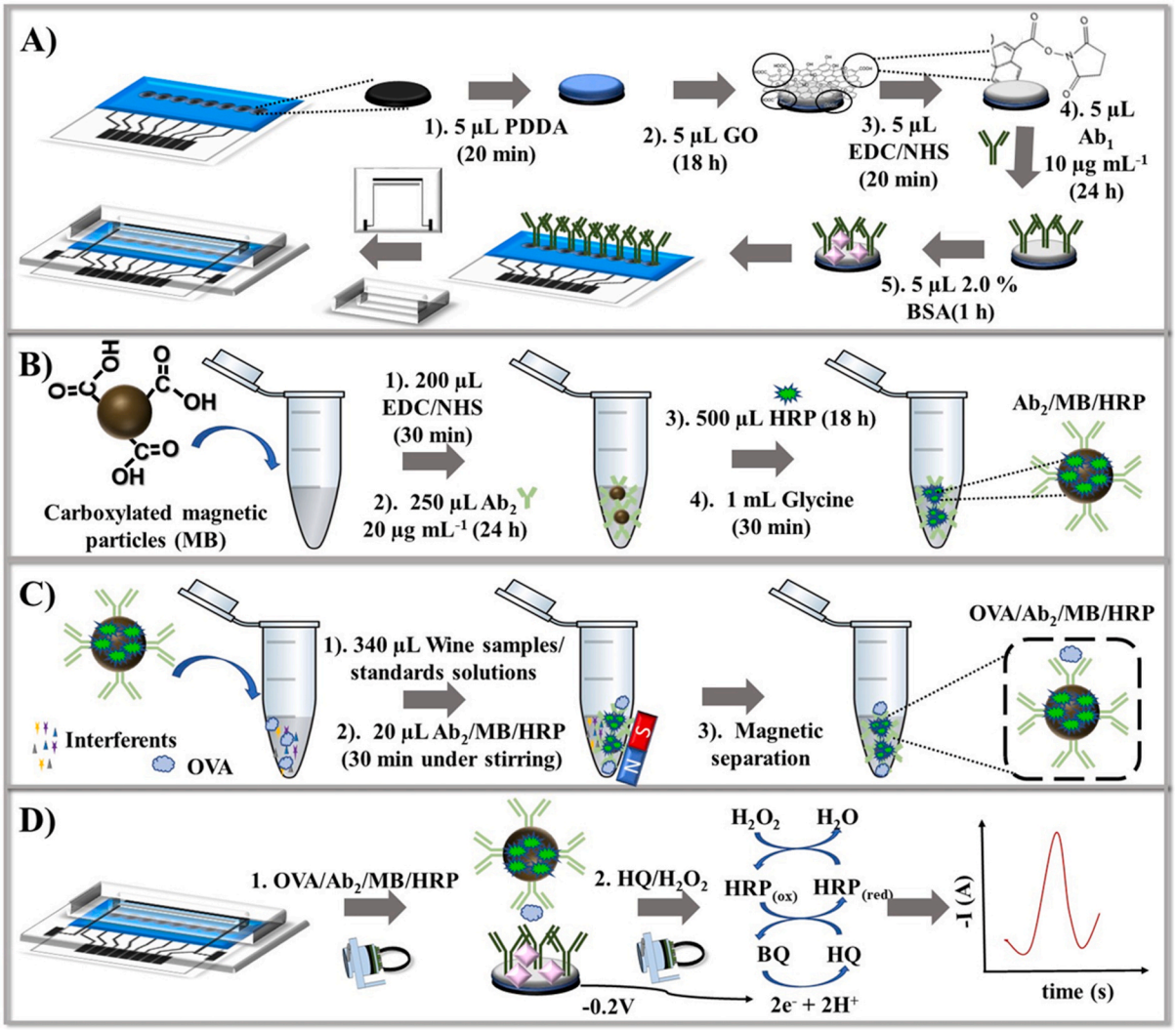


Fig. 2. Schematic illustration of the construction steps of DEμD for OVA detection in wine samples: (A) Modification of 8-WEs with PDDA, GO, covalent immobilization of Ab_1, and the assembling of DEμD; (B) Preparation of the magnetic beads decorated with Ab_2 and HRP; (C) Magneto-immunocapture of OVA, and D) OVA detection by immuno-sandwich formation on DEμD following by the electrochemical measurements.

For covalent immobilization of Ab_2 and HRP, the carboxyl groups present on MBs were activated by adding 200 μL of EDC/NHS to the MBs dispersion (3 mg mL^{-1}) in MES and incubated for 30 min under slow stirring, at room temperature. The MBs were magnetically separated and washed 3 times with MES. In sequence, 250 μL of 20 μg mL^{-1} Ab_2 in MES were added and incubated under slow stirring for 24 h at room

temperature. Subsequently, the conjugated MB-Ab_2 was formed and washed 3 times with 200 μL of MES. To the MBs-Ab_2 formed, 500 μL of HRP (1.2 mg mL^{-1} in PBS) were added and incubated overnight under slow stirring. The resulting bioconjugate Ab_2-MBs-HRP was washed 3 times with 600 μL of PBS, pH 7.0, containing 0.05% Tween-20 (PBS-T20) and 0.1% BSA. Lastly, the remaining activated carboxyl group on MBs were blocked by adding 1.0 mL of 0.1 mol L^{-1}glycine, which was kept in contact for 30 min under slow stirring. Then, the bioconjugate was washed 3 times with PBS-T20 and resuspended in 400 μL of 0.05% PBS-T20 with 0.1% BSA and kept for no longer than 3 weeks at 4 °C until use.

2.6. *Ovalbumin capture, immunosensor formation, and electrochemistry detection using the DEμD*

The method proposed involves the OVA immuno-magnetic capture, its separation from the sample and the injection of the complex formed on the DEμD for immune-sandwich formation at the electrode, followed by the amplified electrochemical detection. To evaluate the immunoassay proposed, 340 μL of the OVA at different concentrations in 0.01 mol L^{-1} PBS and 20 μL of Ab_2-MB-HRP were added in a 2.0 mL microtube and kept under incubation at slow stirring for 30 min at 37 °C. After the capture of the biomarker, the complex formed was separated magnetically and washed 3 times with 400 μL of PBS containing 0.3% BSA (pH 7.0). After the washing step, OVA-Ab_2-MB-HRP bioconjugate was resuspended in 200 μL of PBS-T20 with 0.3% BSA (pH 7.0) and injected in the DEμD. The capture and separation steps are illustrated in Fig. 2C.

In order to generate the immune-sandwich on 8-WEs and evaluate the electrochemical response for OVA detection, a syringe pump was connected to a chromatographic manual injection valve and to the DEμD using polyether ether ketone (PEEK) tubing and connection fittings (Fig. 3). The dispersion with the OVA immuno-magnetically captured was introduced in the injection valve using load mode and filling the 100 μL sample loop. After that, the syringe pump was set at 100 μL min^{-1}, and the dispersion with OVA was injected in the 8-WEs DEμD switching the valve to insert mode. After filling the microchannel, the syringe pump was turned off and kept for different times to allow the immune-sandwich formation (Fig. 2D). After the established time, the syringe pump was turned on and the DEμD was washed with PBS-T20 with 0.1% BSA for 2 min to eliminate the unreacted OVA-Ab_2-MB-HRP. The electrochemical detection was carried out by amperometry by applying a fixed potential of −0.2 V versus Ag|AgCl pseudo reference electrode. The current was recorded when 100 μL of a mixture of 1 μmol L^{-1} H_2O_2 and 20 μmol L^{-1} HQ in PBS (pH 7.0) was injected in the DEμD using the manual injection valve under a flow rate of 100 μL min^{-1}. The solution with HQ and H_2O_2 was purged with nitrogen gas, previously the injection in the microfluidic system. Finally, a transient current response was obtained when the detection solution was injected in the DEμD and the intensity of the peak current was proportional to the OVA concentration. Fig. 2D shows a representative scheme of how the electrochemical detection occurs at each working electrode. The DEμD were checked in every step to avoid bubbles and consequently ensure the feasibility of the method. In the DEμD, the array with 8-WEs (Fig. 1C) was used for eight simultaneous replicates of OVA detection, but it could be applied for detection of up to 8 different analytes by modifying each working electrode with different antibodies for example.

2.7. *Wine sample preparation*

In order to evaluate the feasibility of the immunoassay proposed, the detection of OVA was accomplished in five samples of wine acquired locally. For this, the wine samples were diluted in PBS (pH 7.0) in the proportion of 0.1 mL–200 mL, respectively. The high dilution ratio was performed to minimize matrix effects and to evaluate the ability of the DEμD to detect ovalbumin at low concentrations. Thus, 340 μL of diluted sample was used in the immunoassay developed. The OVA determination was performed by interpolation in the analytical curve.

2.8. *Ovalbumin detection by enzyme-linked immunosorbent assay (ELISA)*

Indirect ELISA was developed for OVA detection in wine samples and used as a comparative method to evaluate the performance of the magneto-immunoassay proposed. OVA standard solutions with concentration from 1.0 ng mL^{-1} to 10 μg mL^{-1} and wine samples were diluted in 0.01 mol L^{-1} of carbonate buffer pH 9.5, then transferred to 96-well polystyrene ELISA plates, where they were kept for 18 h. The wells were washed to remove unbound antigens and 10 μg mL^{-1} of polyclonal anti-OVA antibody previously diluted in PBS-T20 (pH 7.0) was added and kept for 18 h. Next, the wells were washed, and an anti-IgG antibody conjugated with HRP diluted in a 1:15,000 ratio in PBS-T20 was added and kept for 4 h. Following, the unbound HRP-IgG was removed by washing the wells. A 50 μL of commercial solution containing tetramethylbenzidine and H_2O_2 was added and the HRP enzymatic reaction was kept for 15 min at 37 °C and stopped with addition of 0.1 mol L^{-1} HCl. The absorbance of the yellow color originated by the enzymatic reaction was measured at 450 nm. The color intensity was proportional to the concentration of ovalbumin in the samples.

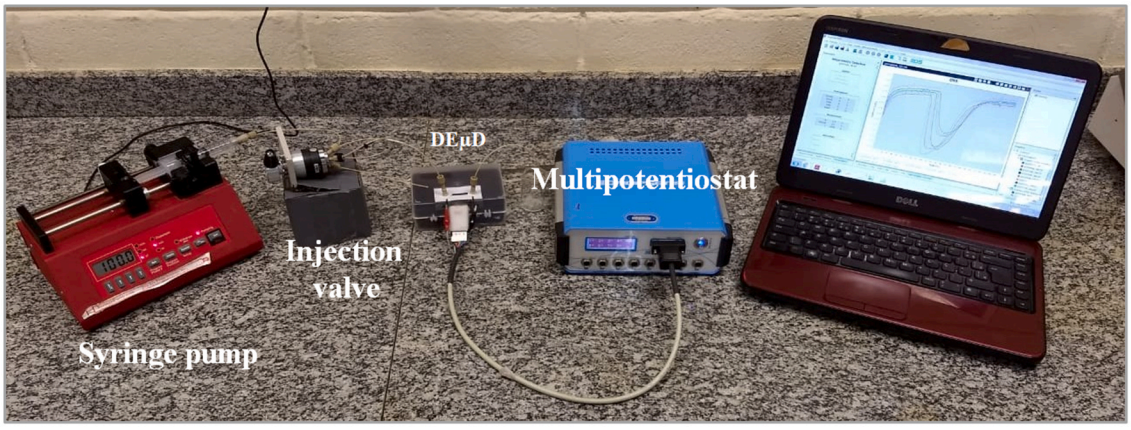


Fig. 3. Microfluidic setup used in the magneto-immunoassay for OVA detection which is composed by a syringe pump, a manual injection valve, the DEμD, and a portable multipotentiostat, connected to a microcomputer for data acquisition.

3. Results

3.1. Characterization of graphene oxide prepared

Raman spectroscopy was utilized for the characterization of graphitic materials, before (Figure S1A in SM) and after (Figure S1B in SM) the GO synthesis. Figure S1 shows the Raman spectra of graphite and GO obtained. For graphite, it is possible to observe two characteristic peaks of raw graphite at 1580 cm^{-1} and a weak peak at 1352 cm^{-1} which corresponds to the G and D bands, respectively. The synthesized material, Figure S1B, showed a shift of the G band to ~1600 cm^{-1} and a significant increase in the intensity of the D band, indicating that sp^2-hybridized carbons were converted to sp^3 state due to the chemical oxidation step. The inset of Figure S1 displays the micrography obtained by scanning electron microscopy (SEM) of the electrode modified with GO, which presents the typical wrinkled structure [20].

3.2. Electrochemical characterization of DEμD constructed

In order to evaluate in how extension GO can improve the electrocatalytic properties of the carbon ink electrodes, the apparent electroactive surface areas of the unmodified DEμD (Fig. 4A) and a DEμD GO modified electrode (Fig. 4B) were determined by cyclic voltammetry at different scan rates and using the Randles-Sevcik equation [28].

$$I_p = \pm (2.69 \times 10^5) n^{3/2} A D^{1/2} C \nu^{1/2} \quad \text{(Eq. 1)}$$

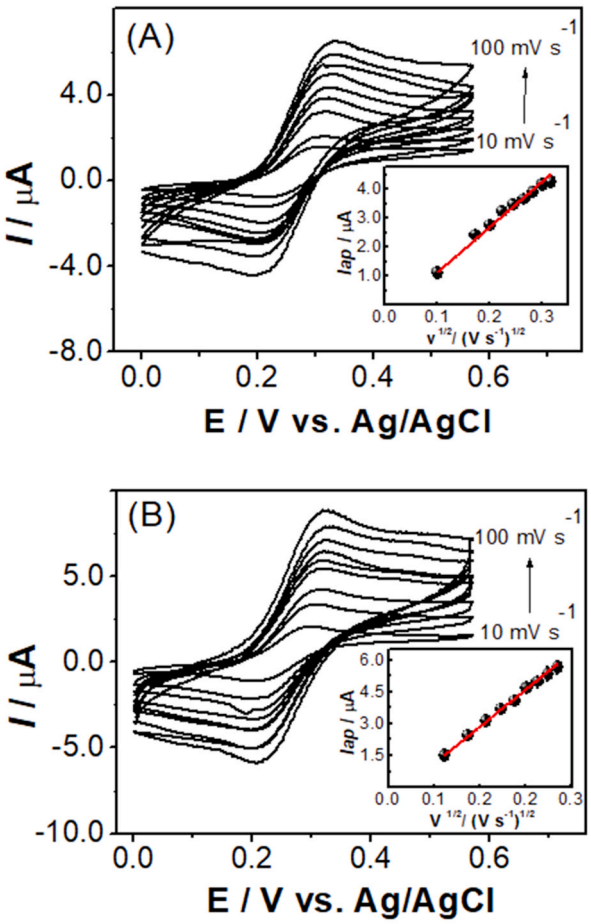


Fig. 4. Cyclic voltammograms of (A) unmodified and (B) GO modified electrodes obtained in 1.0 mmol L^{-1} ferrocene monocarboxylic acid in 0.5 mol L^{-1} KCl. Scan rates of 10, 20, 30, 40, 50, 60, 70, 80, 90, and 100 mV s^{-1}. Insets: Anodic peak current as function of square root of scan rate.

In here, I_p is the peak current; A is the geometric electrode area; n is the number of electrons involved in the reaction; D is the diffusion coefficient; C is the concentration of the redox probe, and ν is the scan rate.

As shown in Fig. 4, the anodic peak currents obtained with both electrodes were proportional to the square root of scan rate, showing that the reaction is controlled by diffusion. According to Eq. (1), the estimated electroactive surface area for the bare carbon-electrode and the GO-modified electrode were 2.44 and 3.36 mm^2, respectively. This means that the presence of GO increased by 38% the voltammetric response in comparison to the bare electrode. There is a consensus that ultra-fast charge mobility processes combined with the high surface-to-volume ratio can favor the analytical signal. Moreover, these properties enable graphene to promote a more effective electron transfer [20].

3.3. Principle of OVA detection by the magnet-immunoassay using DEμD

In the method here proposed, the amount of antibodies immobilized on MBs and the incubation time for both capture and sandwich formation were optimized to obtain the maximum formation of the immune-complex that directly governs the analytical performance of the immunoassay [23,24]. In order to achieve the highest signal for OVA detection, parameters as the concentration of polyclonal anti-OVA antibody applied in the MBs immobilization step, the time required for the incubation between the OVA and MBs decorated with Ab_2, and the time for the sandwich formation on the modified 8-WEs were optimized using PBS solution with a fixed OVA concentration of 50 pg mL^{-1}.

Briefly, the immunoassay proposed involves the OVA immunomagneto capture and separation from sample solution followed by the injection of the immunocomplex formed into DEμD for electrochemical detection based on an immuno-sandwich formation. The steps involved in the magneto-immunoassay are presented in Fig. 2. The first step comprises the immobilization of the antibody anti-OVA on the electrodes of DEμD [25]. After that, as described previously, the DEμD was assembled using a double-side adhesive polystyrene card to attach the modified 8-WEs together with counter and pseudo-reference electrodes and was ready to connect on a chromatographic manual injection valve, as shown at Fig. 3.

The OVA was previously captured by the Ab_2-MB-HRP, after that the OVA-Ab_2-MB-HRP was injected into the DEμD using the microfluidic arrangement [23,25,27]. For this, the sample loop of 100 μL in the manual injection valve was filled with the bioconjugate and then injected into DEμD using the syringe pump at a rate of 100 μL min^{-1}. When OVA-Ab_2-MB-HRP dispersion filled the microfluidic channel, the flow was stopped (time optimized) for immune-sandwich formation due to immunoreaction between the bioconjugate containing the OVA and the Ab_1 immobilized on the 8-WEs. Next, the syringe pump was restarted to wash and eliminated the unbounded OVA-Ab_2-MB-HRP (Fig. 2D). The electrochemical detection was performed by applying a fixed potential of −0.2 V (vs Ag|AgCl) and the injection of a 100 μL of a mixture of 1 μmol L^{-1} H_2O_2 and 20 μmol L^{-1} HQ into the DEμD through the manual injection valve, utilizing a flow rate of 100 μL min^{-1}.

The analytical signal consisted of a transient cathodic current obtained as a function of HQ used as an electrochemical mediator and the HRP enzymatic reaction in presence of subtract (H_2O_2) (Fig. 2D). In this way, when the injected HQ/H_2O_2 solution achieves the electrode with the bioconjugate, the HRP bound to MB reacts with the substrate forming an oxo complex HRP-Fe(IV) = O (HRP_{ox}). Following, the HRP is regenerated to original form HRP_{red} (HRP-Fe(III)) in the presence of HQ forming that oxidase to benzoquinone (BQ). Finally, the BQ was electrochemically reduced to HQ at the electrode surface and the transient current was registered. The electrochemical detection is indirect, because the antigens and antibodies do not exhibit redox behavior (Fig. 2D). The magnitude of the cathodic current obtained is proportional to the OVA concentration. In the current study, different parameters of the magneto-immunoassay proposed were evaluated to achieve the best analytical performance for OVA detection.

3.4. Optimization of the magnet-immunoassay for OVA detection using DEμD

The use of magnetic beads decorated with primary antibody and HRP allowed the capture and separation of the OVA from sample solution, diminishing drastically the interference derived from the matrix effect. The formation of an immune-sandwich structure on the electrode with the immobilized secondary antibody and the bioconjugate containing the captured OVA, allowed an amplification of the analytical signal due to the presence of multiple HRPs linked to the MB for each OVA bound on the immobilized antibody on the electrode. Together with these strategies to improve the selectivity and sensitivity for OVA detection, the quantity of antibody immobilized on MB and the times involving the immunoreactions are important parameters that affect the analytical performance of the assay. Based on this premise, the quantities of Ab_2 immobilized on MBs and the time applied in the incubation for OVA capture in sample solution and in the immune-sandwich formation on the DEμD were evaluated.

The first parameter evaluated was the concentration of antibodies used to prepare the decorated magnetic beads. For this, concentrations of antibodies in the interval of 5–40 μg mL^{-1} were used and the modified MBs obtained were applied for detection of 50 pg mL^{-1} of OVA. In this optimization step, a time of 30 min was used in the immuno-capture and in the sandwich formation steps, following previous works [23,25]. Fig. 5A presents the influence of Ab_2 concentration in the cathodic current obtained for OVA detection. The amount of Ab_2 immobilized on magnetic beads influences the quantity of OVA bound and consequently there is an optimal quantity of OVA to be immuno-magnetically captured. As it can be seen, the cathodic peak current obtained increased up to 20 μg mL^{-1}, followed by a slight decrease in the signal for higher concentrations. Therefore, 20 μg mL^{-1} Ab_2 was used in the further experiments.

The influence of the time for the OVA magneto-immunocapture was evaluated in the interval of 10–40 min. The transient current obtained for the detection of 50 pg mL^{-1} of OVA using different immunocapture times are presented in Fig. 5B. As can be seen, 30 min resulted in the highest peak current response in comparison with the other times studied and this was the time selected for the following experiments. Finally, the time for immune-sandwich formation on the electrode in DEμD was evaluated. Reaction time of 10, 20, 30, 40, 50, and 60 min for a detection of 50 pg mL^{-1} of OVA, were evaluated and the results are presented in Fig. 5C. In this case, the highest value for the transient current was obtained at 20 min, indicating that this relatively short time was enough to assemble a higher number of immunocomplexes on the

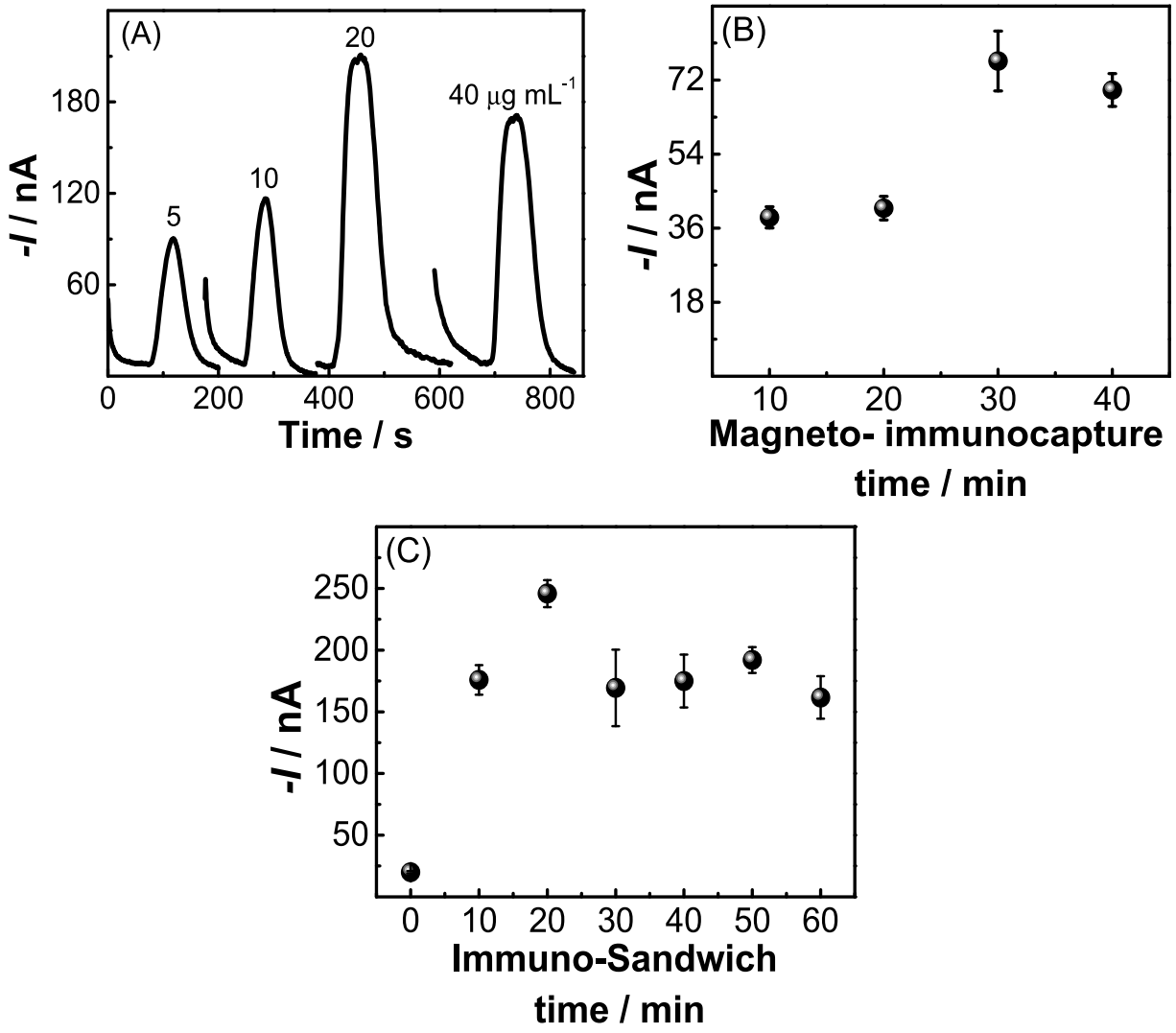


Fig. 5. **(A)** Effect of Ab_2 concentrations (5, 10, 20, and 40 μg mL^{-1}) on cathodic current responses for detection of 50 pg mL^{-1} of OVA. **(B)** Influence of the time applied (10, 20, 30, and 40 min) in the magneto-immunocapture of OVA on the current response. **(C)** Influence of the time applied in the immuno-sandwich formation (10, 20, 30, 40, 50, and 60 min) at DEμD for OVA detection. Experiments carried in PBS-T-20 buffer (pH 7.0) and $E_{ap} = -0.2$ V; [OVA] = 50 pg mL^{-1}; [Ab_1] = 10 μg mL^{-1}; [HQ] = 20 μmol L^{-1}; [H_2O_2] = 1 μmol L^{-1}, and n = 5 (number of electrodes at the DEμD used for these studies).

electrode surface. Longer times caused a decrease in the current signal, which may be related to partial inactivation of the antibodies, decreasing the overall analytical response of the immunosensor. In the following studies the concentration of Ab_2 of 20 μg mL^{-1}, 30 min for the magneto-immunocapture, and 20 min for the formation of the immune-sandwich was adopted. The concentration of Ab_1 and the number of units of HRP used were chosen based on previous works [23,25].

3.5. Analytical performance and the OVA detection in wine samples

Under the optimized conditions, the performance of the proposed immunoassay was evaluated at different concentrations of OVA in standard solutions. A new DEμD was used for each concentration and it was disposed of after use. As can be seen in Fig. 6A, increasing transient cathodic currents were produced when the OVA concentration increased. A good linear response was obtained in the range of 0.01–10 pg mL^{-1} of OVA with a sensitivity of 41 nA mL pg^{-1} (Fig. 6B). The synergistic effect of MPs heavily decorated with Ab_2 and HRP for capture and separation of OVA and the presence of GO on the electrode allowed to achieve an ultralow limit of detection (LoD) of 0.2 fg mL^{-1} for this immunoassay. The LoD was calculated by (3.3 *s*)/*b*, where *s* is the standard deviation of the blank (n = 10) and *b* is the slope of the calibration curve.

The repeatability of the disposable DEμD was evaluated for the OVA detection at concentration of 0.01 pg mL^{-1}. The relative standard deviations (RSD) values obtained using the same 8-WEs DEμD was 5,9%, while three different DEμD resulted in RSD value of 7,0%. These results

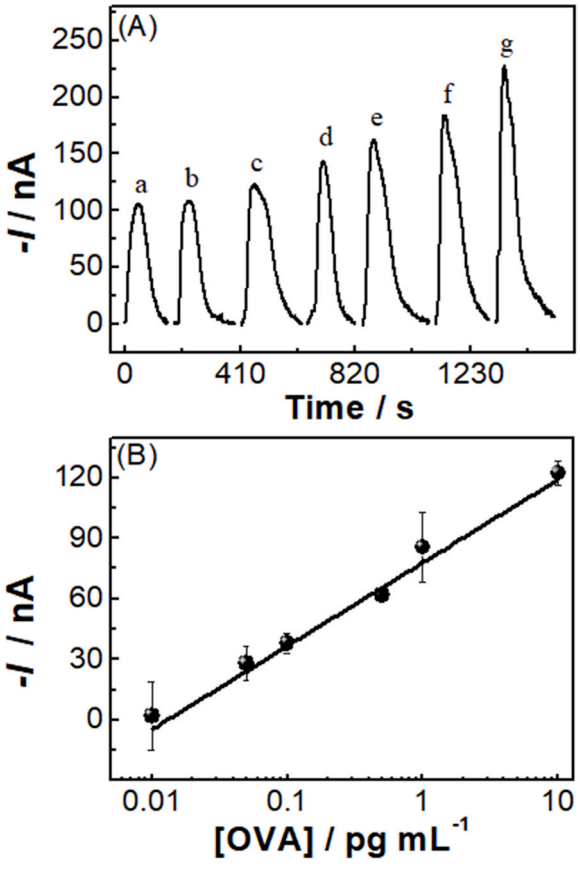


Fig. 6. (A) Transient current responses for different concentrations of OVA obtained with the DEμD. (a) 0; (b) 0.01; (c) 0.05; (d) 0.1; (e) 0.5; (f) 1.0 and (g) 10 pg mL^{-1} of OVA. (B) Dependence of the peak current on log of OVA concentration. Other conditions: $[Ab_1]$ = 10 μg mL^{-1}; $[Ab_2]$ = 20 μg mL^{-1}; [HQ] = 20 μmol L^{-1}; and $[H_2O_2]$ = 1.0 μmol L^{-1} prepared in PBS-T20 buffer (pH 7.0). E_{ap} = −0.2 V.

confirmed the efficient repeatability and reproducibility of the method proposed for the ultrasensitive OVA detection.

The results obtained with the developed magneto-immunoassay were compared with other works in the literature for OVA detection and are presented in Table 1. As can be seen, the limit of detection obtained in this work is the lowest compared with other electrochemical immunosensors previously reported.

As can be seen in Table 1, the immunoassay developed presented a wide linear range for OVA determination with an ultralow limit of detection, in comparison to other electrochemical biosensors reported in the literature. Other advantageous aspects are disposability, specificity, low cost, and user-friendliness. Čadková et al. [31] presented an immunosensor for ovalbumin determination using magnetic beads (MBs) exhibiting linear responses in the range from 0.5 to 9.5 μg mL^{-1}. In this work, MBs enable the capture of OVA from complex biological samples. An immune-sandwich structure was formed on the MBs, not on the electrode, using commercial anti-OVA IgG labeled with HRP. The use of this strategy limits the relation to 1:1 from OVA and HRP restricting the LoD. In our strategy, the large number of HRP present on decorated MBs [23,24] associated with the use of a GO modified electrode produces an amplified electrochemical response, allowing to achieve a large linear range and ultralow LoD. Although the proposed method has a higher number of operation steps when compared to the others mentioned in Table 1, the DEμD allows to carry out eight simultaneous analyses with a total assay time of 60 min. Other advantages of the DEμD for OVA detection developed in this study include the simple fabrication process, the need of only a few microliters of sample, and the possibility of easy automation. Moreover, the immunoassay proposed based on use of magnetic beads and DEμD can be easily modified for simultaneous detection of other proteins as allergens in foods.

The stability of the Ab_1 on 8-WEs screen-printed array modified with PDDA and GO was also evaluated. For this, different Ab_1-modified arrays were prepared on the same day and stored at 4 °C in PBS (See Fig. S2 in SM). The DEμDs were tested in different days for the detection of ovalbumin in standard solution at 1.0 pg mL^{-1}. The device showed a decrease in the transient current responses obtained of 5.1%, after three days. After longer times of storage the stability of the immunosensor was reduced, retaining 86% and 71% of the initial analytical performance after 5 and 10 days of storage, respectively. In this way, the immobilization of Ab_1 on 8-WEs screen-printed array modified with PDDA and GO showed good stability. The study was carried out with the electrode kept in PBS solution, however, a longer shelf-life for immunoassays is expected when they are kept under dry conditions.

In order to evaluate the feasibility of the DEμD for OVA determination in food samples, the developed protocol was tested toward this biomarker in red and white wines and compared with ELISA. Fig. 7 and Table S1 presented the results for OVA detection using the magneto-immunoassay and ELISA. For both methods, the OVA concentration was obtained by interpolation in the calibration curve.

As can be seen, the red wines showed higher levels of OVA compared to white wines. In both cases, the results obtained with the method here developed presented excellent agreement with values obtained using ELISA in parallel analysis. The results obtained by both methods showed a correlation of 0.985 with *p*-value (0.2) of paired *t*-test indicating no difference in the confidence level of 95%, showing a calculated *t* (1.0) much lower than critical value from *t* (2.1).

Therefore, the magneto-immunoassay proposed showed remarkable and fast results for cost-effective OVA determination in real samples of wines. Our device allowed eight simultaneous analyses with a cost of less than U$ 1.00 in material per device, which is lower than ELISA (comparative method), and a cost about USD 5.25 per microwell.

4. Conclusions

This study described the combination of a fully disposable

Table 1
Comparison of the performance of different electrochemical immunoassays used for the detection of OVA.

Sensing substrate	Technique	Linear range	LoD	Assay time (min)	Number of steps	Reference
GO/screen printed carbon	Differential pulse voltammetry	1 pg mL^{-1} - 0.5 μg mL^{-1}	0.83 pg mL^{-1}	60	5	[29]
Dextran-coated sensor chips (CM5)	surface plasmon resonance (SPR)	0.03–0.2 μg mL^{-1}	0.6 μg mL^{-1}	–	4	[30]
Screen printed platinum	Linear sweep voltammetry	0.5–9.5 μg mL^{-1}	0.2 μg mL^{-1}	60	4	[31]
Graphene/screen printed carbon electrodes	Amperometry	0.01–10 pg mL^{-1}	0.2 fg mL^{-1}	60	6	This work

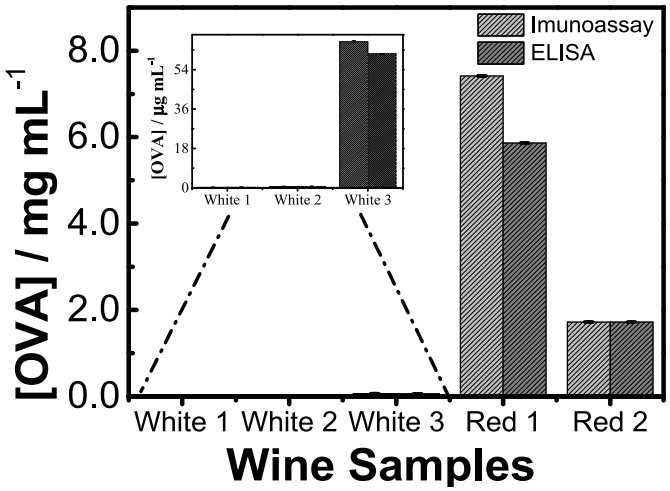


Fig. 7. Comparison of the OVA detection using the magneto-immunoassay proposed and ELISA in wine samples.

electrochemical microfluidic device with magnetic beads for the development of a magneto-immunoassay for ultrasensitive detection of egg allergen ovalbumin in food samples. The DEμD developed in our lab allows until 8 simultaneous detections per device. The electrodes were modified with graphene oxide to favor the covalent immobilization of Ab_1. The structure obtained was highly favorable for the detection of OVA, providing high sensitivity with LoD of 0.2 fg mL^{-1} and wide linear range of concentration from 0.01 to 10 pg mL^{-1}. Additional advantages of the DEμD developed in this study were its easy and simple construction with excellent reproducibility and cost-effective scalability. The proposed method was successfully applied for OVA determination in samples of white and red wines showing results with excellent agreement with results obtained by ELISA. Finally, the magneto-immunoassay strategy developed in this study can be easily adapted for fast and simple detection of other proteins as allergens in foods and drinks.

5. Credit author statement

Thaisa Aparecida Baldo: Conceptualization; Data curation; Formal analysis; Investigation; Methodology; Software; Validation; Visualization; Writing - original draft. Camila dos Anjos Proença: Conceptualization; Data curation; Formal analysis; Investigation; Methodology; Software; Validation; Visualization; Writing - original draft. Fabiana da Silva Felix: Conceptualization; Data curation; Investigation; Methodology; Writing - review & editing. Tayane Aguiar Freitas: Conceptualization; Data curation; Investigation; Methodology; Writing - review & editing. Solange Kazumi Sakata: Conceptualization; Investigation. Lucio Angnes: Resources; Funding acquisition; Writing - review & editing; Ronaldo Censi Faria: Conceptualization; Resources; Funding acquisition; Project administration; Supervision; Writing - review & editing.

Declaration of competing interest

The authors declare that they have no known competing financial interests or personal relationships that could have appeared to influence the work reported in this paper.

Acknowledgements

The authors gratefully acknowledge financial support provided by CAPES (Finance Code No# 001), CNPq (Proc. No. 308570/2018–9 and 311847-2018-8), and FAPESP (2013/14262–7, 2016/00991–5, 2017/24053–7, 2017/13137–5) and FAPESP /INCT (2014/50867–3).

Appendix A. Supplementary data

Supplementary data to this article can be found online at https://doi.org/10.1016/j.talanta.2021.122447.

References

[1] N. Ahsan, R.S.P. Rao, P.A. Gruppuso, B. Ramratnam, A.R. Salomon, Targeted proteomics: current status and future perspectives for quantification of food allergens, J. Proteomics 143 (2016) 15–23, https://doi.org/10.1016/j.jprot.2016.04.018.
[2] S. Kirsch, S. Fourdrilis, R. Dobson, M.-L. Scippo, G. Maghuin-Rogister, E. De Pauw, Quantitative methods for food allergens: a review, Anal. Bioanal. Chem. 395 (2009) 57–67, https://doi.org/10.1007/s00216-009-2869-7.
[3] J.M. Rolland, E. Apostolou, M.P. de Leon, C.S. Stockley, R.E. O'Hehir, Specific and sensitive enzyme-linked immunosorbent assays for analysis of residual allergenic food proteins in commercial bottled wine fined with egg white, milk, and nongrape-derived tannins, J. Agric. Food Chem. 56 (2008) 349–354, https://doi.org/10.1021/jf073330c.
[4] A. Lifrani, J. Dos Santos, M. Dubarry, M. Rautureau, F. Blachier, D. Tome, Development of animal models and sandwich-ELISA tests to detect the allergenicity and antigenicity of fining agent residues in wines, J. Agric. Food Chem. 57 (2009) 525–534, https://doi.org/10.1021/jf8024584.
[5] R. Pilolli, L. Monaci, Challenging the limit of detection for egg allergen detection in red wines by surface plasmon resonance biosensor, Food Anal. Methods. 9 (2016) 2754–2761, https://doi.org/10.1007/s12161-016-0464-z.
[6] J.B. Roses, Food allergen law and the Food Allergen Labeling and Consumer Protection Act of 2004: falling short of true protection for food allergy sufferers, Food Drug Law J. 66 (2011) 225–242. http://www.ncbi.nlm.nih.gov/pubmed/24505841. (Accessed 13 September 2019).
[7] E. Parliament, Regulation (EU) 1169/2011 of the European Parliament and of the Council of 25 October 2011 on the provision of food information to consumers, Off J Eur Union (2011) 304–318 (EC) No,that may mislead the consumer, https://eur-lex.europa.eu/LexUriServ/LexUriServ.do?uri=OJ:L:2011:304:0018:0063:EN:PDF#targetText=According to Regulation. (Accessed 13 September 2019).
[8] F. Castellucci. Resolution OIV/OENO 427/2010 Criteria for the Methods of Quantification of Potentially Allergenic Residues of Fining Agent Proteins, International Organisation of Vine and Wine: OIV, 2010.
[9] R. Madrid, S. de la Cruz, A. García-García, M.J.C. Alcocer, I. González, T. García, R. Martín, Multimeric recombinant antibody (scFv) for ELISA detection of allergenic walnut. An alternative to animal antibodies, J. Food Compos. Anal. 67 (2018) 201–210, https://doi.org/10.1016/J.JFCA.2018.01.017.
[10] Z. Gao, Y. Ma, X. Zhou, Z. Yang, H. Jia, L. Gao, S. Wu, L. Han, X. Yi, H. Wang, J. H. Akkerdaas, R. van Ree, Quantification of peach fruit allergen lipid transfer protein by a double monoclonal antibody-based sandwich ELISA, Food Anal. Methods. 9 (2016) 823–830, https://doi.org/10.1007/s12161-015-0272-x.
[11] J. Xi, Q. Shi, Development of an indirect competitive ELISA kit for the detection of soybean allergenic protein gly m bd 28K, Food Anal. Methods. 9 (2016) 2998–3005, https://doi.org/10.1007/s12161-016-0493-7.
[12] C. Koestel, C. Simonin, S. Belcher, J. Rösti, Implementation of an enzyme linked immunosorbent assay for the quantification of allergenic egg residues in red wines using commercially available antibodies, J. Food Sci. 81 (2016) T2099–T2106, https://doi.org/10.1111/1750-3841.13378.

[13] P. Weber, H. Steinhart, A. Paschke, Investigation of the allergenic potential of wines fined with various proteinogenic fining agents by ELISA, J. Agric. Food Chem. 55 (2007) 3127–3133, https://doi.org/10.1021/jf063436s.
[14] V. Ruiz-Valdepeñas Montiel, R.M. Torrente-Rodríguez, S. Campuzano, A. Pellicanò, A.J. Reviejo, M.S. Cosio, J.M. Pingarrón, Simultaneous determination of the main peanut allergens in foods using disposable amperometric magnetic beads-based immunosensing platforms, Chemosensors 4 (2016) 1–14, https://doi.org/10.3390/chemosensors4030011.
[15] A.J. van Hengel, Food allergen detection methods and the challenge to protect food-allergic consumers, Anal. Bioanal. Chem. 389 (2007) 111–118, https://doi.org/10.1007/s00216-007-1353-5.
[16] M.L. Downs, P. Johnson, Target selection strategies for LC-MS/MS food allergen methods, J. AOAC Int. 101 (2018) 146–151, https://doi.org/10.5740/jaoacint.17-0404.
[17] V. Di Stefano, G. Avellone, D. Bongiorno, V. Cunsolo, V. Muccilli, S. Sforza, A. Dossena, L. Drahos, K. Vékey, Applications of liquid chromatography–mass spectrometry for food analysis, J. Chromatogr. A 1259 (2012) 74–85, https://doi.org/10.1016/J.CHROMA.2012.04.023.
[18] I.-H. Cho, J. Lee, J. Kim, M. Kang, J. Paik, S. Ku, H.-M. Cho, J. Irudayaraj, D.-H. Kim, Current technologies of electrochemical immunosensors: perspective on signal amplification, Sensors 18 (2018) 1–18, https://doi.org/10.3390/s18010207.
[19] I.J. Dinshaw, S. Muniandy, S.J. Teh, F. Ibrahim, B.F. Leo, K.L. Thong, Development of an aptasensor using reduced graphene oxide chitosan complex to detect Salmonella, J. Electroanal. Chem. 806 (2017) 88–96, https://doi.org/10.1016/J.JELECHEM.2017.10.054.
[20] F.S. Felix, L.M.C. Ferreira, F. Vieira, G.M. Trindade, V.S.S.A. Ferreira, L. Angnes, Amperometric determination of promethazine in tablets using an electrochemically reduced graphene oxide modified electrode, New J. Chem. 39 (2015) 696–702, https://doi.org/10.1039/C4NJ00887A.
[21] S.K. Krishnan, E. Singh, P. Singh, M. Meyyappan, H.S. Nalwa, A review on graphene-based nanocomposites for electrochemical and fluorescent biosensors, RSC Adv. 9 (2019) 8778–8781, https://doi.org/10.1039/c8ra09577a.
[22] J. Peña-Bahamonde, H.N. Nguyen, S.K. Fanourakis, D.F. Rodrigues, Recent advances in graphene-based biosensor technology with applications in life sciences, J. Nanobiotechnol. 16 (2018) 75, https://doi.org/10.1186/s12951-018-0400-z.
[23] C.V. Uliana, C.R. Peverari, A.S. Afonso, M.R. Cominetti, R.C. Faria, Fully disposable microfluidic electrochemical device for detection of estrogen receptor alpha breast cancer biomarker, Biosens. Bioelectron. 99 (2018) 156–162, https://doi.org/10.1016/j.bios.2017.07.043.
[24] R.A.G. De Oliveira, E.M. Materon, M.E. Melendez, A.L. Carvalho, R.C. Faria, Disposable microfluidic immunoarray device for sensitive breast cancer biomarker detection, ACS Appl. Mater. Interfaces 9 (2017) 27433–27440, https://doi.org/10.1021/acsami.7b03350.
[25] C.A. Proença, T.A. Baldo, T.A. Freitas, E.M. Materón, A. Wong, A.A. Durán, M. E. Melendez, G. Zambrano, R.C. Faria, Novel enzyme-free immunomagnetic microfluidic device based on Co0.25Zn0.75Fe2O4 for cancer biomarker detection, Anal. Chim. Acta 1071 (2019) 59–69, https://doi.org/10.1016/J.ACA.2019.04.047.
[26] R. Malhotra, V. Patel, B.V. Chikkaveeraiah, B.S. Munge, S.C. Cheong, R.B. Zain, M. T. Abraham, D.K. Dey, J.S. Gutkind, J.F. Rusling, Ultrasensitive detection of cancer biomarkers in the clinic by use of a nanostructured microfluidic array, Anal. Chem. 84 (2012) 6249–6255, https://doi.org/10.1021/ac301392g.
[27] T.A. Freitas, C.A. Proença, T.A. Baldo, E.M. Materón, A. Wong, R.F. Magnani, R. C. Faria, Ultrasensitive immunoassay for detection of Citrus tristeza virus in citrus sample using disposable microfluidic electrochemical device, Talanta 205 (2019) 120110, https://doi.org/10.1016/J.TALANTA.2019.07.005.
[28] J.F. Rusling, K. Ito, Voltammetric determination of electron-transfer rate between an enzyme and a mediator, Anal. Chim. Acta 252 (1991) 23–27, https://doi.org/10.1016/0003-2670(91)87192-A.
[29] S. Eissa, L. L'Hocine, M. Siaj, M. Zourob, A graphene-based label-free voltammetric immunosensor for sensitive detection of the egg allergen ovalbumin, Analyst 138 (2013) 4378–4384, https://doi.org/10.1039/c3an36883a.
[30] R. Pilolli, A. Visconti, L. Monaci, Rapid and label-free detection of egg allergen traces in wines by surface plasmon resonance biosensor, Anal. Bioanal. Chem. 407 (2015) 3787–3797, https://doi.org/10.1007/s00216-015-8607-4.
[31] M. Čadková, R. Metelka, L. Holubová, D. Horák, V. Dvořáková, Z. Bílková, L. Korecká, Magnetic beads-based electrochemical immunosensor for monitoring allergenic food proteins, Anal. Biochem. 484 (2015) 4–8, https://doi.org/10.1016/j.ab.2015.04.037.